Energy Equip. Sys./ Vol. 13/No. 3/September 2025/ 363-380

ENERGY EQUIPSYS

Energy Equipment and Systems

www.energyequipsys.com

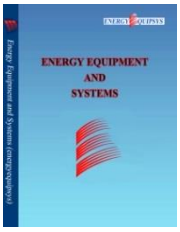

Numerical study of the temperature distribution of combustion products in different parts of the fire-tube boilers to evaluate boiler steam generation

Manuscript Type
Research Paper

Authors

Maryam Hassani[a]
Mahtab Askari[b]
Ramin Kouhikamali[c*]

[a] Damadej Espadan Company, Isfahan, Iran

[b] Faculty of Mechanical Engineering, University of Guilan, Rasht, Iran

[c] Department of Mechanical Engineering, Isfahan University of Technology, Isfahan, Iran

Article history:
Received: 15 February 2025
Revised: 19 March 2025
Accepted : 23 April 2025

ABSTRACT

In this research, a three-pass fire tube boiler has been numerically simulated in order to investigate the temperature distribution of combustion products in different parts of a sample boiler. The turbulent flow of the flame and combustion products is simulated by the finite volume approach by using the Discrete Ordinates model to simulate radiation and the Species Transport model to simulate the combustion phenomenon. Each part has been separately simulated with inlet characteristics of the outlet of the last part, and the smoke temperature distribution in each part has been presented. In addition, effective parameters of burner capacity, furnace type (corrugated or plain), furnace and tube length, and diameter have been studied on the temperature distribution of combustion product and boiler performance. According to the obtained results, with increasing the length by 55% or diameter by 54% of the furnace, steam production increases by 6.56% and 1.5% respectively. By corrugating the furnace, the gas outlet temperature reduces and the boiler capacity of steam production increases. Reducing the diameter of the tubes by 20% and increasing the length of the tubes by 25% in the 2nd pass and 18% in the 3rd pass (with the same heat transfer surface of the tubes in pass 2 and 3), leads to steam production increase by 3% and 1.68%, respectively. Results showed that for a larger proportion of 3rd pass tubes, boiler performance increases. Also, increasing in the burner capacity (by 33%) leads to the same value increase in the steam production.

Keywords: Fire-Tube Boiler; CFD Simulation; Geometrical Study; Boiler Performance; Burner Capacity; Temperature Distribution.

1. Introduction

Fire-tube boilers are one of the main equipment of thermal power plants, which generally consist of a combustion chamber and smoke tubes. Combustion product produced from fuel burning in boiler furnace passes through furnace(s) and reversal chamber(s) as the first pass and smoke tubes of second and third passes, and heats and evaporates surrounding water with pool boiling mechanism. The pass in a fire tube boiler represents the gas proceeding in the boiler length. In 3-pass fire tube boilers

* Corresponding author: Ramin Kouhikamali
Department of Mechanical Engineering, Isfahan University of Technology, Isfahan, Iran
Email: r.kouhikamali@iut.ac.ir

which are the most conventional in the industry, the furnace is assumed as the first pass, and the second and third passes are considered for smoke tubes. It is obvious that the temperature of hot gases from combustion decreases during passing through the boiler, which means that heat is transferred to the water around the furnace and the tube bundles, resulting in water boiling and saturated steam production.

Different research have been carried out on fire tube boilers. Ortiz [1] presented a dynamic analysis for predicting fire-tube boiler performance by using MATLAB software. He considered most of the effective physical parameters in his model, which made it applicable for boiler designing. Makishi et al. [2] investigated the effect of scale on the inner surface of the boiler tube on its thermal resistance by calculating tube temperature rise. Mahmoudi et al. [3] presented a computational fluid dynamics simulation and the exergy analysis of a sample fire-tube boiler and compared the results of both analyses with actual operational values. Bisetto et al. [4] carried out an empirical analysis and modeling of fire-tube boilers with 3 passes. Abene et al. [5] presented a transient simulation of the hydraulic behavior of a 3-pass fire-tube boiler during a cold start-up, based on the energy balance equations. The wall temperature and heat transfer rate in all three passes was studied and an acceptable agreement between the experimental data and the simulation results was found. Beyne et al. [6, 7] modeled fire-tube boiler by consideration of submerged and non-submerged reversal chambers based on the steady state and dynamic models of plug flow furnace with experimental correlations and ε-NTU with and without radiation inclusion. They used the steady state model for design optimization and dynamic model for calculation of boiler peak load capability. They also studied reversal chamber placement effects. In the plug flow furnace model, they presented the temperature graph and showed that the temperature of the gas in the first pass is high due to combustion and reaches a maximum value, then its temperature decreases while passing through the second and third passes. At the tube bundles in the second and third passes, the gas temperature distribution is similar to full convective heat transfer profile, which indicates the importance of convective heat transfer compared to radiation heat transfer in smoke tubes. Khostov et al. [8] utilized Ansys-Fluent software in order to simulate the hydrodynamics characteristic of fire-tube boilers. Lahijani et al. [9] investigated the efficiency of fire-tube boilers by using an indirect heat loss method and found three of the most effective parameters on the efficiency of steam boilers including flue gas temperature, ambient temperature and type of fuel. Gaćeša et al. [10] studied the effect of furnace shape, such as corrugated furnaces with different depth and pitch, on thermal stress in fire-tube boilers by the finite element method. They found that with increasing in the depth of corrugating in corrugated furnaces, thermal stresses significantly decrease and in the boilers with high steam production capacity, corrugated furnaces must be used to increase the equipment lifetime. Tognoli et al. [11] presented a dynamic model of an industrial fire-tube boiler. The performance of five different geometries of some existing boilers was also studied in their research. They found that using higher capacity boilers has no advantages related to the other cases from the view point of controllability, and smaller capacity boilers can also be used to provide the customer's steam demand. Also, in another study [12], they modeled a fire-tube boiler equipped with reverse flow combustor and they got similar results regarding the use of higher capacity boilers. Rahmani and Trabelsi [13] modeled 4-pass fire tube boilers and after validating the model in comparison with experimental data, the effect of pressure drop on gas temperature, thermal heat flux, heat transfer coefficient, wall temperature and heat transfer rate were studied in different passes. Kute [14] investigated the heat transfer in two types of plain and helically ribbed tubes of a fire-tube boiler. She states that by using helically ribbed tubes, heat transfer rate and boiler efficiency increases. Mohammadi et al. [15] numerically investigated a heat exchanger to utilize energy of the combustion products from the boiler. Jha and Lele [16] developed a model consists of a transient heat transfer and hydrodynamic calculations. They calculated heat transfer and water wall temperature in order to calculate gas temperature, gas and water heat transfer. Morelli et al. [17] provided a heat transfer coefficient correlation for hot water fire tube

boilers based on one-dimensional finite volume approach. In addition, they simulated the thermo-physical behavior of the gas inside the fire tubes. They [18], in addition to the hot water boiler sizing by simulating gas behavior, predicted the outlet hot water temperature by using machine learning algorithms. Kotb and Saad [19] developed a mathematical model in order to predict the performance of fire tube boiler. Pilali et al. [20] optimized thermal design of an industrial 3-pass fire tube boiler with an internal super heater and determined the influence of different parameters on the outlet temperature of super-heated steam.

Fire tube boilers are practical equipment in industrial applications. They produce saturated steam in a two-phase pool boiling phenomena heated by radiation and convection heat transfer mechanisms of the flow of combustion products of air and fuel generated in boiler furnace. In comparison with the previous work, this study simulates exact and point to point phenomena of combustion and heat transfer in three passes of the fire tube boiler. These complex phenomena are modeled numerically in order to analyze flow hydrodynamics, heat transfer and effective parameters on the boiler performance. In this research by using Computational Fluid Dynamics (CFD), a three-pass fire-tube boiler is numerically simulated in real dimensions and operating conditions. The main objective of this research is to investigate the temperature distribution of combustion products in different parts of the boiler (Furnace and the smoke tubes of the 2nd and 3rd passes) and conduct parametric studies to discover the more effective ones on steam production capacity.

Nomenclature

E	Total energy (J)
$\vec{F}$	Force vector (N)
h	Enthalpy (J/kg)
h^0	Enthalpy of formation (J/kmol)
J	Diffusion flux (kg/m^2-s)
k	Conductivity (W/m-K)
M	Molar mass (kg/kmol)
$\dot{m}$	Mass flow rate (kg/s)
P	Pressure (Pa)
R	volumetric rate of creation (kg/m^2-s)
$\vec{s}$	Direction vector (m)
S_h	Source term of chemical reaction (J/m^2-s)
S_r	Source term of radiation (J/m^2-s)
T	Temperature (K)
$\vec{V}$	Overall velocity vector (m/s)
Y	Mass fraction (-)

Greek letters

μ	Dynamic viscosity (Pa-s)
ρ	Density (kg/m^3)
$\bar{\tau}$	Stress tensor (Pa)

Subscripts

eff	effective
i	Inlet
j	Species index
o	Outlet
1	First pass
2	Second pass
3	Third pass

2. Modeling

A fire tube boiler is modeled numerically in order to evaluate boiler performance and its steam generation. A base case and influences of different parameters, including burner capacity, furnace geometry, and tube heat surface, are studied based on conservation laws and the finite volume approach of numerical modeling.

2.1. Problem definition

The current problem is a 3-pass, 1-furnace fire-tube boiler with geometrical characteristics presented in Table 1 as the base case. It can be seen that the tube surfaces of the 2nd and the 3rd pass consist of around 36% and 57% of all heating surfaces of the base case study.

Table 1. Geometrical characteristics of the base case, studied fire-tube boiler

	Quantity	Length (m)	Diameter (mm)	Thickness (mm)
Furnace	1	2	600	16
2nd pass	48	2	60.3	3.2
3rd pass	54	2.8	60.3	3.2

The boiler burner has a heating capacity of 2.4 MkCal/hr and can produce 3 ton/hr saturated steam. Geometrical and schematic characteristics of the base case of the fire tube boiler is shown in Fig. 1. The fuel from the burner center mixes with the air coming at an angle of 45°. Mass flow rate of air and fuel can be calculated with the fuel heating value, burner heating capacity, and mass ratio of air to fuel.

In order to study effective parameters on the temperature distribution of combustion products, the following parameters and conditions are studied:

1. Different capacities of burners, including burners with 1.8, 2.0, 2.2 and 2.4 MkCal/hr capacities that for each the mass flow rate of combustion products also changes.
2. Different furnace geometries, including a corrugated furnace with pitch and depth of 115 and 30 mm, respectively, plain furnaces with constant length of 2 m for outside diameter of 0.45, 0.5, 0.7, and 0.7 m and constant outside diameter of 0.6 m for lengths of 1.2, 1.5, 2.5 and 3.0 m
3. Different 2nd and 3rd pass tube numbers, including constant tube diameter for different tube lengths and constant tube length for different tube diameters, in such a way that tube surface areas remain constant by changing their quantity, as the following table (Table 2)

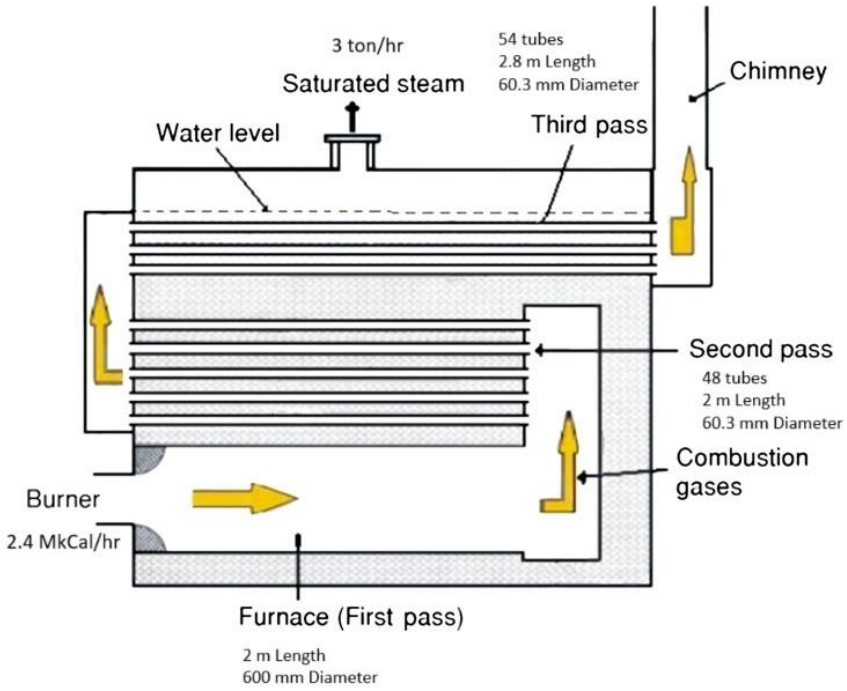

Fig. 1. Geometrical and schematic characteristics of the base case of fire tube boiler

Table 2. Different case studies for investigating the effects of tubes geometry

Tube outer diameter (mm)	Tube length (m)		Tube number		Tube distribution (%)	
	2nd pass	3rd pass	2nd pass	3rd pass	2nd pass	3rd pass
48	2.0	2.8	60	68	40	60
75	2.0	2.8	39	43	40	60
60	1.5	2.3	64	66	40	60
60	2.5	3.3	38	46	40	60
60	2.0	2.8	62	44	50	50
60	2.0	2.8	75	35	60	40

In the current problem, combustion phenomena in the furnace and radiation heat transfer mechanism, in addition to turbulence of combustion and combustion product flow, are considered.

2.2. Governing equations

The steady state governing equations of the problem are described as follows [21]:

Conservation of mass:

$$\nabla.\left(\rho\vec{V}\right)=0 \tag{1}$$

In which, ρ is the density and $\vec{V}$ is the flow overall velocity.

Conservation of momentum without consideration of gravity:

$$\nabla.\left(\rho\vec{V}\vec{V}\right)=-\nabla P+\nabla.\bar{\tau}+\vec{F} \tag{2}$$

where P is the pressure, μ is the dynamic viscosity, and $\vec{F}$ is the force vector. $\bar{\tau}$ The stress tensor as following:

$$\bar{\tau}=\mu\left[\left(\nabla\vec{V}+\nabla\vec{V}^{T}\right)-\frac{2}{3}\nabla.\vec{V}I\right] \tag{3}$$

Conservation of energy:

$$\nabla.\left(\vec{V}\left(\rho E+P\right)\right)= \nabla.\left(k_{eff}\nabla T-\sum_{j}h_{j}J_{j}+\bar{\tau}.\vec{V}\right)+S_{h}+S_{r} \tag{4}$$

In Eq. (4), E is the total energy, k_{eff} is the effective thermal conductivity, T is the temperature, h_j and J_j are j^{th} species enthalpy and diffusion flux, respectively and S_h and S_r show the energy source due to chemical reaction (the creation rate by addition from the dispersed phase) and radiation, respectively. S_h is defined as the following:

$$S_{h}=-\sum_{j}\frac{h_{j}^{0}}{M_{j}}R_{j} \tag{5}$$

where h_j^0, R_j and M_j is the enthalpy of formation, volumetric rate of production by chemical reaction, and molar mass of species j, respectively.

Conservation of chemical species [22]:

$$\nabla.\left(\rho\vec{V}Y_{j}\right)=-\nabla.\left(J_{j}\right)+S_{hj}+R_{j} \tag{6}$$

For modeling mixing of chemical components of fuel and air (Y_j as the mass fraction of species j), it is assumed that they are mixed in a molecular scale and therefore they have common velocity, pressure, and temperature fields.

In order to calculate the mass fraction of each species, natural gas is considered as the fuel of the boiler with consideration of 30% excess air (based on the information of the burner supplier) as the following reaction relation:

$$\begin{aligned}&0.965CH_4+0.013N_2+0.017C_2H_6\\&+0.001C_3H_8+0.001C_4H_{10}+0.003CO_2\\&+2.6013\left(O_2+3.76N_2\right)+1.111439429H_2O\\&\rightarrow\ 1.009CO_2+3.101439429H_2O\\&+9.793888N_2+0.6003O_2\end{aligned} \tag{7}$$

Air relative humidity is considered 87% and the creation rate of chemical reaction is defined by the Eddy dissipation model [23].

Radiation heat transfer mechanism of high-temperature combustion products is solved based on the Discrete Ordinates (DO) Model [24]. This model solves the radiative transfer equation for a finite number of discrete solid angles of $\vec{s}$ direction vector.

In order to simulate turbulence in the furnace and tubes of passes 2 and 3, RNG k-ε and standard k-ε is used respectively. k-ε turbulent model is used by different researchers for the simulation of combustion [24-25].

Boundary conditions are presented in Table 3, and the simulated geometrical characteristics of furnace and tubes of the 2nd and 3rd passes are presented in Fig. 2.

2.3. Numerical simulation

Numerical simulation of the current study has been carried out in three steps indicated in Fig. 3. In this figure, indices of i, o, 1, 2 and 3 correspond to inlet, outlet, first pass, second pass and third pass, respectively; T_{i1} is the temperature of inlet fuel and air, T_{o3} is the outlet temperature of combustion product from boiler and $\dot{m}$ shows the combustion product mass flow rate.

Table 3. Boundary conditions of the current problem

Part	Boundary	Characteristic	Value
Furnace	Fuel inlet	Mass flow rate (kg/s)	0.0574
		Temperature (K)	333
		Components mole fraction	CH_4: 0.965, N_2: 0.013, C_2H_6: 0.017, C_3H_8: 0.001, C_4H_{10}: 0.001, CO_2: 0.003
	Air inlet	Mass flow rate (kg/s)	1.31649
		Temperature (K)	333
		Components mole fraction	O_2: 0.1927, H_2O: 0.08236, N_2: 0.72494
	Outlet	Pressure (Pa)	0 gauge
		Components	Air-fuel mixture
	Wall surface	Temperature (K)	473.15
2nd pass	Inlet	Mass flow rate (kg/s)	0.02862 for each tube
		Temperature (K)	Outlet of furnace
	Outlet	Pressure (Pa)	0 gauge
		Components	Air-fuel mixture
	Wall surface	Temperature (K)	473.15
3rd pass	Inlet	Mass flow rate (kg/s)	0.02544 for each tube
		Temperature (K)	Outlet of the 2nd pass
	Outlet	Pressure (Pa)	0 gauge
		Components	Air-fuel mixture
	Wall surface	Temperature (K)	473.15

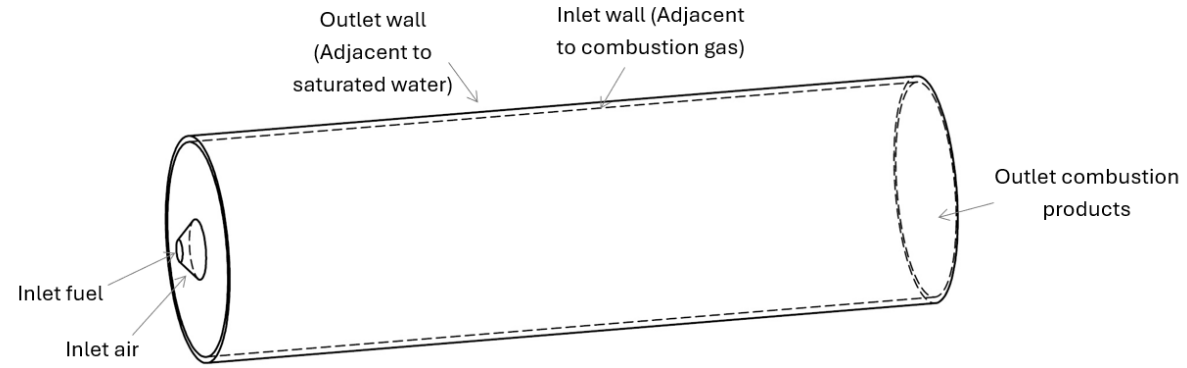

(a)

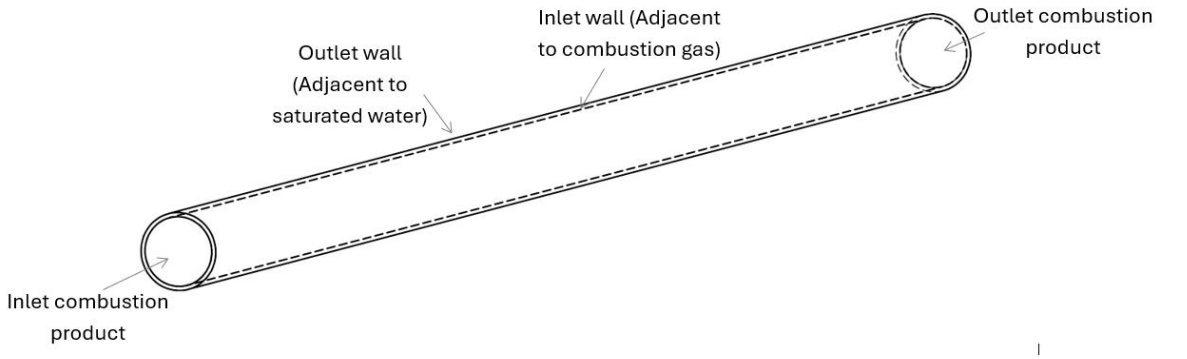

(b)

Fig. 2. Geometrical characteristics of (a) furnace and (b) tube of 2nd and 3rd pass

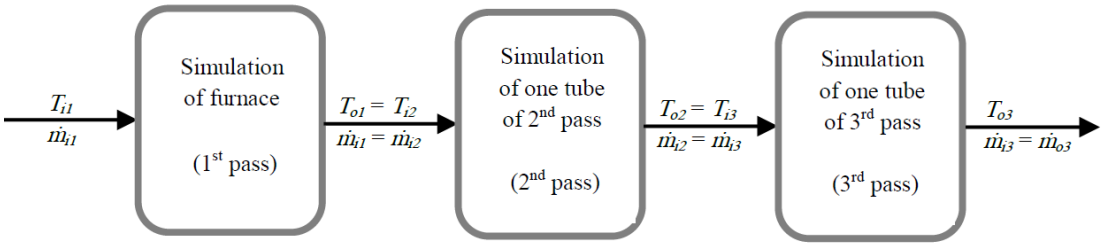

Fig. 3. Simulation steps of the current problem

The current problem has been solved by the finite volume approach of the commercial CFD code of Ansys Fluent 19.1. For the simulation of turbulence in the furnace and tubes of the 2nd and 3rd passes, RNG k-ε and standard k-ε models are utilized, respectively. Radiation heat transfer mechanism is simulated by the DO radiation model [24], and combustion phenomenon is modeled by the use of Species Transport model in which the absorption coefficient of air-fuel mixture is considered by Weighted Sum of Gray Gas Model (WSGGM) [26-28].

Air-fuel mixture density and specific heat capacity is calculated based on incompressible ideal gas and mixing law formula of the mixture, respectively. In addition, stainless steel is considered as the material of furnace and tubes.

In order to pressure-velocity coupling, SIMPLE algorithm is utilized. For discretization of pressure, momentum, energy, turbulent kinetic energy and turbulent energy dissipation, PRESTO! and 2nd order upwind scheme has been used.

As indicated in Fig.4, boiler furnace is meshed with unstructured grid of polyhedral type and the tubes of the 2nd and 3rd passes are meshed with structured grid of hexahedral type.

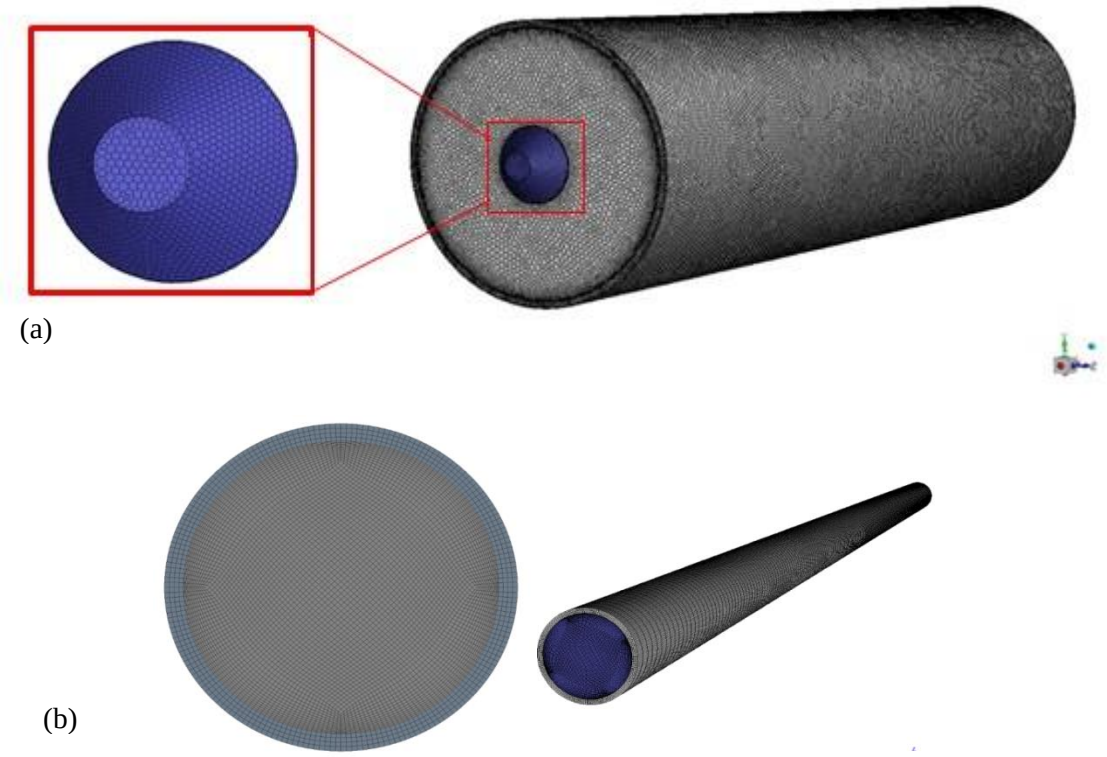

Fig. 4. Grid of (a) furnace and (b) tubes of 2nd and 3rd pass of boiler

The independence procedure of grid from the result is presented in Fig. 5, in which three different grids are studied for furnace and tubes of pass 2 and 3 and temperature distribution of combustion products is studied along the length. According to Fig. 5, the grids with 868386, 1335699 and 1864800 cells, respectively for furnace and tubes of pass 2 and 3, due to the small deviation of the value of combustion products temperature with the smaller cell number are selected as the final grids for study.

The independence procedure of grid for all other mentioned cases of section 2-1 has been carried out and related results are presented for the mesh independent ones.

3. Results and discussion

Issues including model verification, results of the based studied case and investigation of the influences of diffident parameters such as burner capacity, geometrical characteristics of the furnace and 2nd and 3rd pass tubes are discussed in this section.

3.1. Model verification

For validation of the current numerical model, the boiler experimental data of Rahmani and Dahia [29] are compared with the results of the current numerical simulation for the experimental geometrical and operating conditions. The compared results are indicated in Table 4. The comparison of the results indicates good agreement of the numerical prediction with the experimental data with a maximum 13.5% deviation of the outlet temperature of combustion products of the boiler.

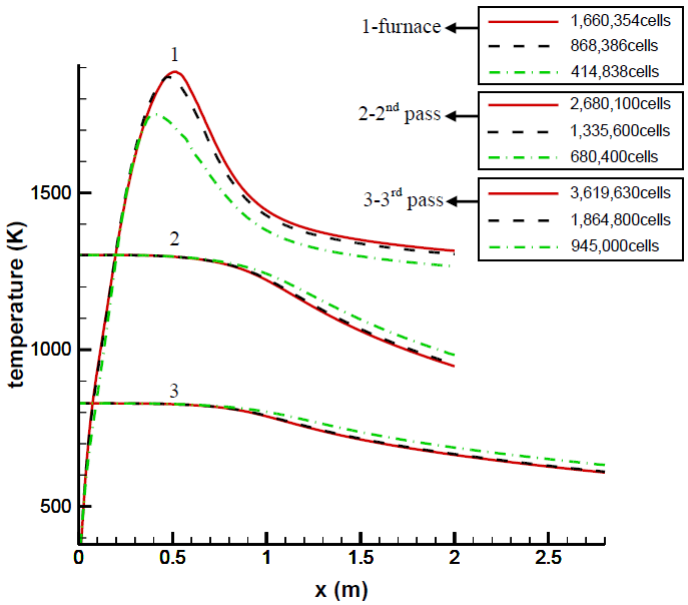

Fig. 5. Independence procedure of grid from for furnace and tubes of 2nd and 3rd pass of boiler

Table 4. Comparison of the results of the current numerical simulation with the experimental data of Rahmani and Dahia [29]

Operating pressure (bar)	Mass flow rate of combustion products (kg/s)	Excess air percent (%)	Outlet gas temperature from the 3rd pass (K)		
			Current numerical simulation	Experimental data [29]	Deviation (%)
0.5	0.0275	7.1	174.9	154	13.5
3.0	0.0275	7.0	185.1	184	0.59
3.5	0.0275	6.9	190.4	188	1.2
4.0	0.0275	4.0	195	190	2.6
6.0	0.055	3.8	230.2	219	5.1
6.75	0.055	3.7	233.6	228	2.4

3.2. Base case results

Figure 6 shows the temperature contour of combustion and generated combustion products in the central plate of the plain furnace of the base case. As indicated in this figure, adiabatic flame temperature and outlet temperature of the furnace are 1906 and 1302 K, respectively.

Outlet temperature of combustion products from passes 2 and 3 is 828.7 and 572.4 K, respectively. This boiler has the steam production capacity of 3 ton/hr in which the furnace and 2nd and 3rd passes have the portions of 50.4%, 32.7% and 16.9%, respectively. In addition, the overall results of heat transfer of the base case are represented in Table 5. It clearly shows the higher proportion of radiation heat transfer mechanism in the furnace.

3.3. Effect of burner capacity and length, and diameter of furnace

The effect of furnace diameter, furnace length, and burner capacity on temperature of boiler passes and heat transfer rate (overall, radiation and convection) are shown in Fig. 7(a-c) and Fig. 8(a-c), respectively.

By increasing furnace surface area, either by its diameter or length, the outlet temperature of combustion products from the furnace and tubes of 2nd and 3rd passes decreases, which describes heat transfer increasing. Due to the high temperature of gas in boiler furnace (around 1900 K of flame adiabatic temperature), the radiation heat transfer mechanism is dominant (Fig. 8 shows). By increasing the surface area of the furnace, according to Fig. 6, gas velocity decreases, and the portion of convective heat transfer decreases and the increase of heat transfer is caused by the increase of radiation heat transfer. As Fig. 7(c) and 8(c) show, increasing burner capacity increases mass flow rates of combustion products and their velocity in the furnace and tubes, which leads to decreasing gas outlet temperature and increasing convection, radiation, and total heat transfer.

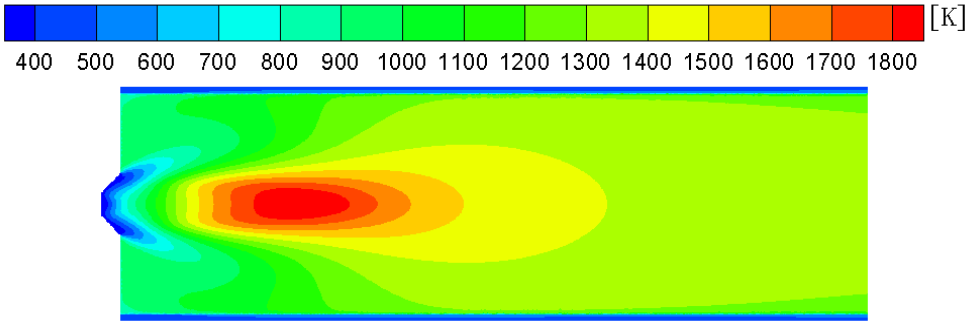

Fig. 6. Temperature contour of combustion and combustion products in the central plate of the plain furnace

Table 5. Heat transfer results for the base case of the boiler

	Furnace	2nd pass	3rd pass
Total heat transfer (kW)	1089.4	708.3	364.9
Radiation heat transfer (kW)	820.2	--	--
Convection heat transfer (kW)	269.2	--	--
Convection heat transfer coefficient (W/m^2-K)	223	61.2	
Pressure drop (Pa)	486.9	85.1	99.1
Steam production portion (%)	50.4	32.7	16.9

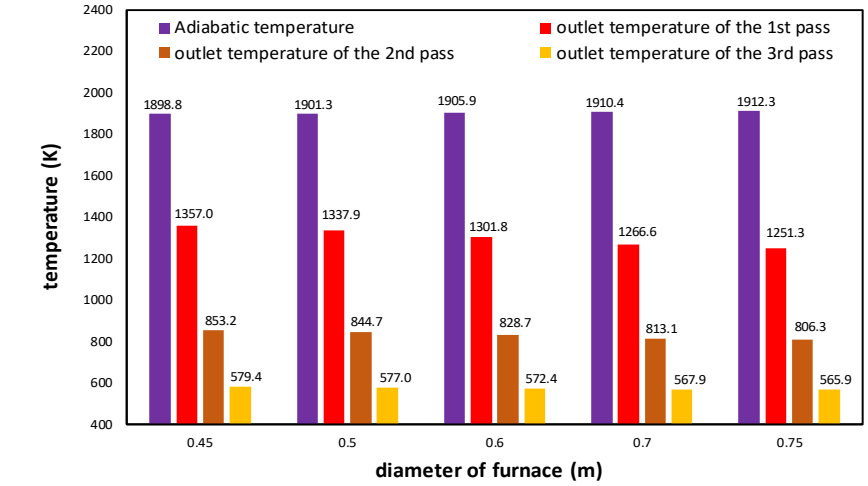

(a)

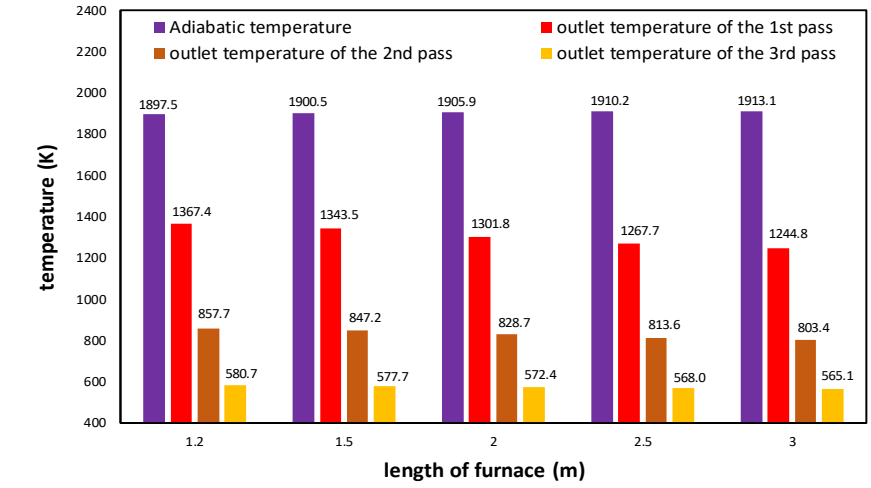

(b)

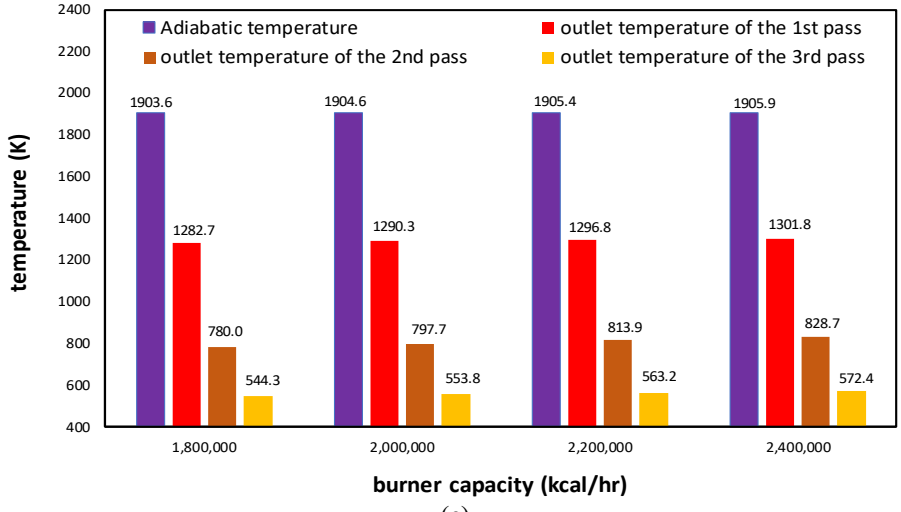

(c)

Fig. 7. Effect of (a) furnace diameter, (b) furnace length and (c) burner capacity on temperature of boiler passes

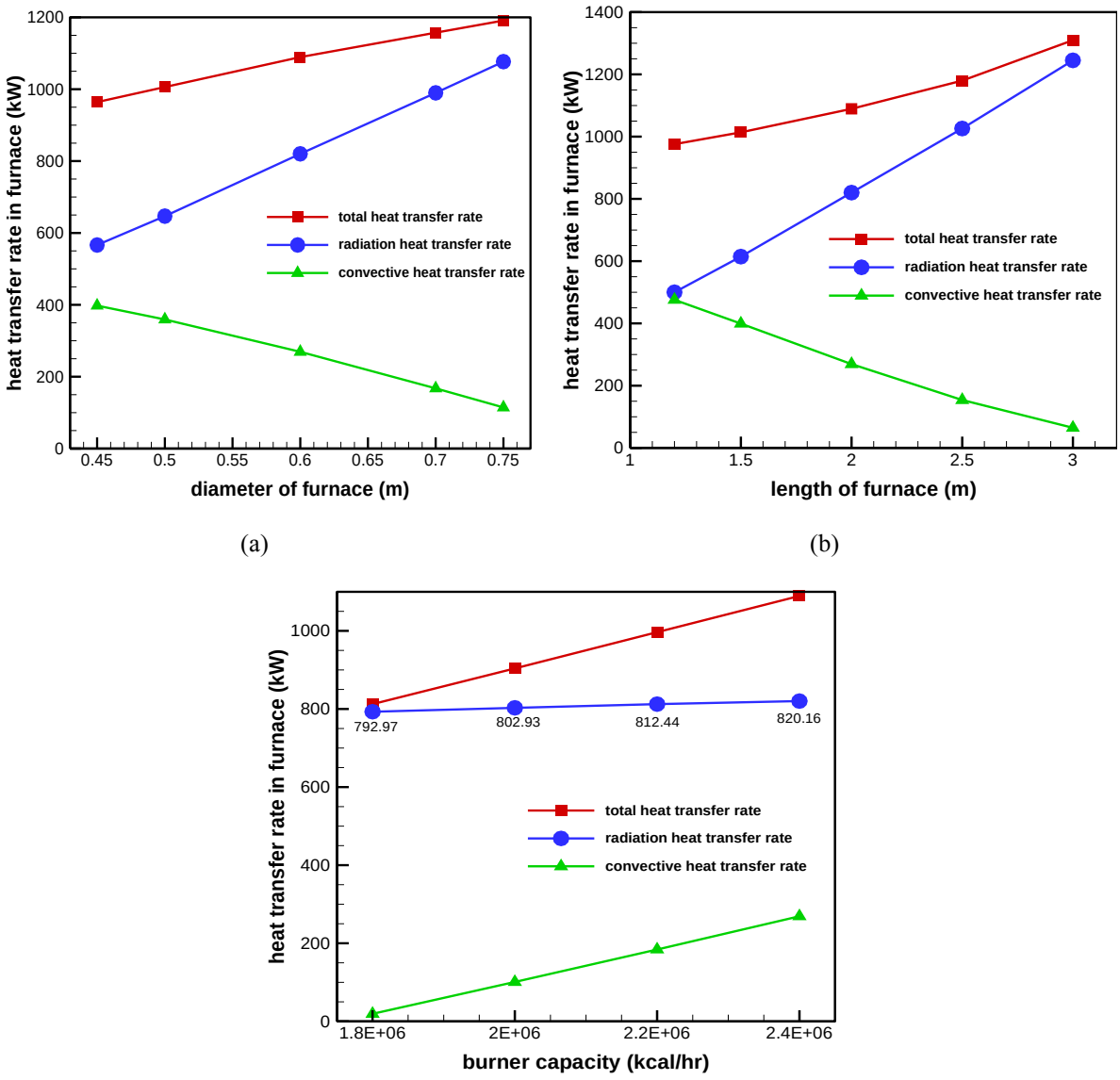

Fig. 8. Effect of (a) furnace diameter, (b) furnace length and (c) burner capacity on heat transfer rate

Figure 7 represents the total heat transfer coefficient and pressure drop of the furnace by changing the furnace diameter, length, and burner capacity.

Increasing the gas temperature difference causes a decrease in the value of boiler component logarithmic temperature difference (LMTD). Therefore, an increase of the surface of the boiler, a decrease of its LMTD and an increase of total heat transfer have leaded to an increase of total heat transfer coefficient shown in Fig. 9(a).

According to Fig. 9(a), pressure drop in furnace is decreased by increasing furnace diameter and is increased by increasing furnace length which can be clearly explained by Darci-Weisbach equation. Increasing burner capacity, in constant dimension of furnace and increased mass flow rate and velocity of combustion products has increased the pressure drop.

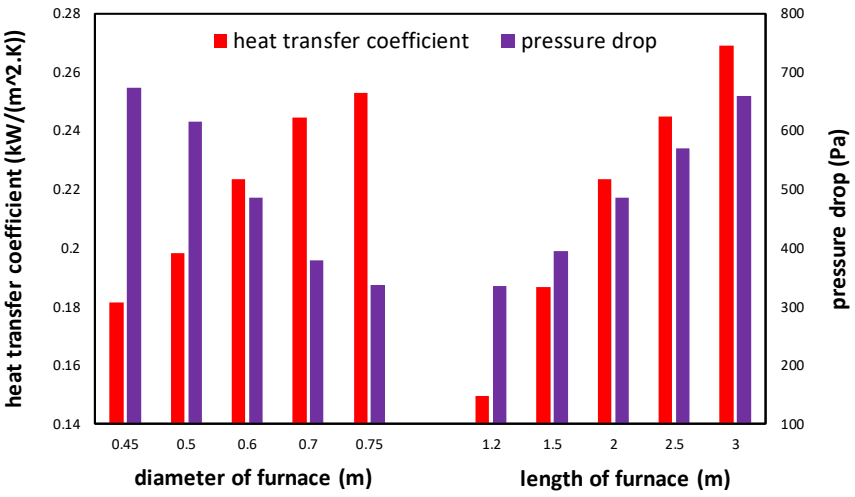

(a)

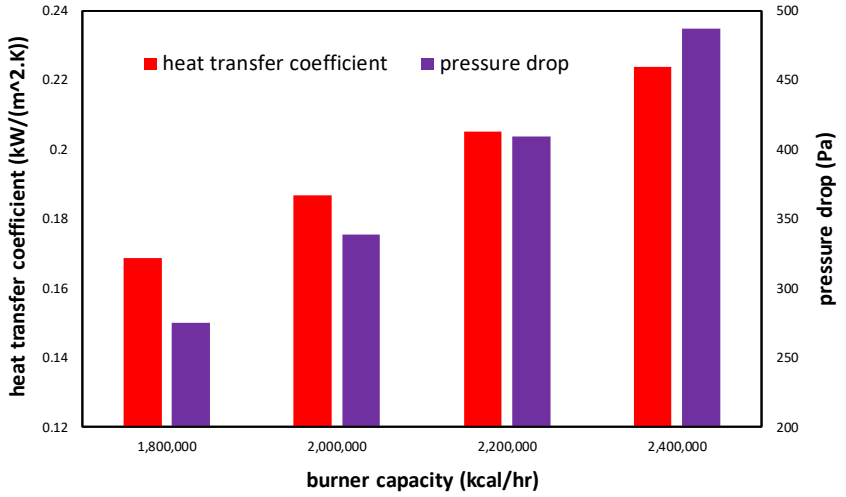

(b)

Fig. 9. Effect of (a) furnace diameter and furnace length and (b) burner capacity on heat transfer coefficient and pressure drop

In other words, increase of furnace length and burner capacity leads to increase of total heat transfer coefficient and pressure drop. While increase of furnace diameter increases total heat transfer coefficient with decreasing pressure drop.

Fig. 10 compares generated steam mass flow rate by increasing furnace diameter and length and burner capacity. By increasing furnace diameter and length, although heat transfer in the 2nd and 3rd passes has decreased due to lower inlet gas temperature, higher total heat transfer causes greater production of steam. Bigger burner capacity also increases heat power and generated steam.

Increase and decrease percent of generated steam in studied cases in comparison with the base case is also indicated in Fig. 10. Increasing burner capacity has a more significant effect on steam production capacity. Increasing 55% of furnace surface area by its length increases steam production by 6.56% and increasing 29% of furnace surface area by its diameter increases steam production by 1.5%. This is while burner power increase of 33%, causes steam production increase to 33%.

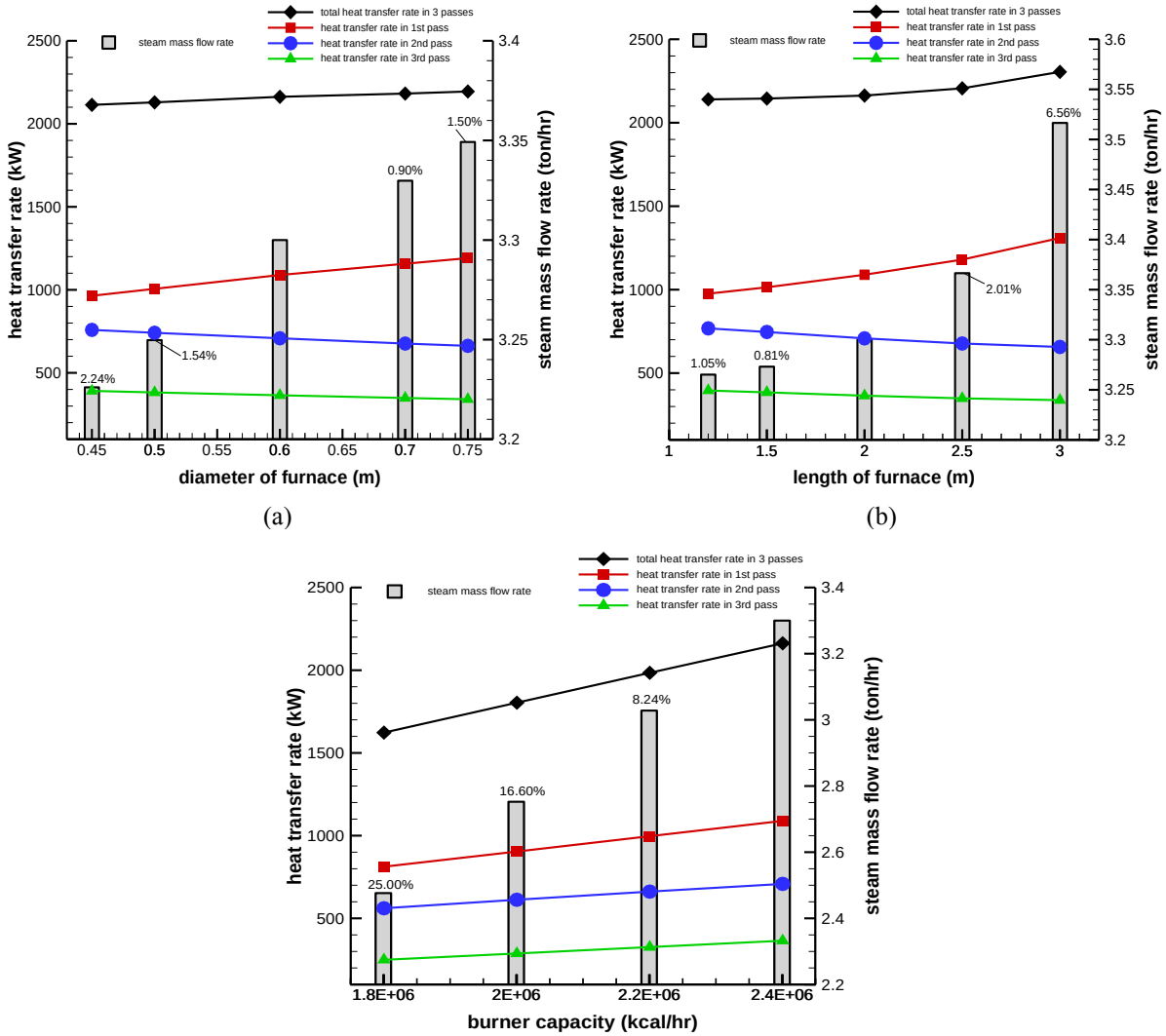

Fig. 10. Effect of (a) furnace diameter, (b) furnace length and (c) burner capacity on heat transfer rate and steam production

3.4. Effect of corrugated furnace

Table 6 represents the effect of the corrugated furnace.

Corrugation has led to a decrease of outlet temperature from the 3 passes and more heat transfer in the furnace. Therefore, the heat transfer coefficient and steam generation in the furnace increase. Increasing furnace surface area by corrugation decreases the convection portion and increases radiation portion of heat transfer. According to Table 6, corrugating doesn't have a significant effect on steam production capacity. But it is a sufficient way to increase thermal and mechanical strength of the furnace, especially for high capacity boilers.

3.5. Effect of the length and diameter of the smoke tube and their distribution

The effects of changing 2nd and 3rd pass tube diameter and length, and their distribution on the temperature of gas and heat transfer rate are indicated in Fig. 11 and Fig. 12, respectively. With increasing tube diameter, the outlet temperature of gas from the 2nd and 3rd passes increases, which means that temperature variation along tubes decreases, which causes a lower heat transfer rate. A reverse result is seen for increasing tube length. According to Figs 11 and 12, tube distribution of 40-60% in the 2nd and 3rd passes has led to lower outlet temperature of the 3rd pass and higher heat transfer rate.

Table 6. The results of corrugating the furnace

Characteristic	Value	Characteristic	Value
Flame adiabatic temperature (K)	1909.5	Total heat transfer rate in furnace (kW)	1140.1
Outlet temperature of furnace (K)	1274.2	Radiation heat transfer rate in furnace (kW)	946.4
Outlet temperature of 1st pass (K)	816.5	Convection heat transfer rate in furnace (kW)	193.8
Outlet temperature of 2nd pass (K)	568.9	Heat transfer coefficient in furnace (kW/m^2-K)	0.2373
Heat transfer rate in 1st pass (kW)	683.2	Pressure drop in furnace (Pa)	500.7
Heat transfer rate in 2nd pass (kW)	351.8	Steam mass flow rate (ton/hr)	3.32
Total heat transfer rate in 3 passes (kW)	2175.2	Increase of steam production (%)	0.58

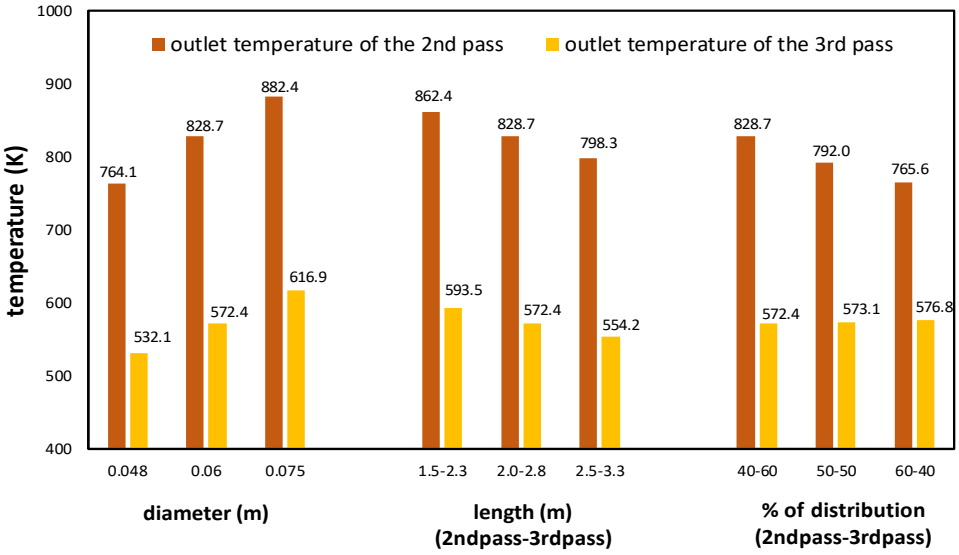

Fig. 11. Effect of tube diameter, length and distribution on temperature distribution

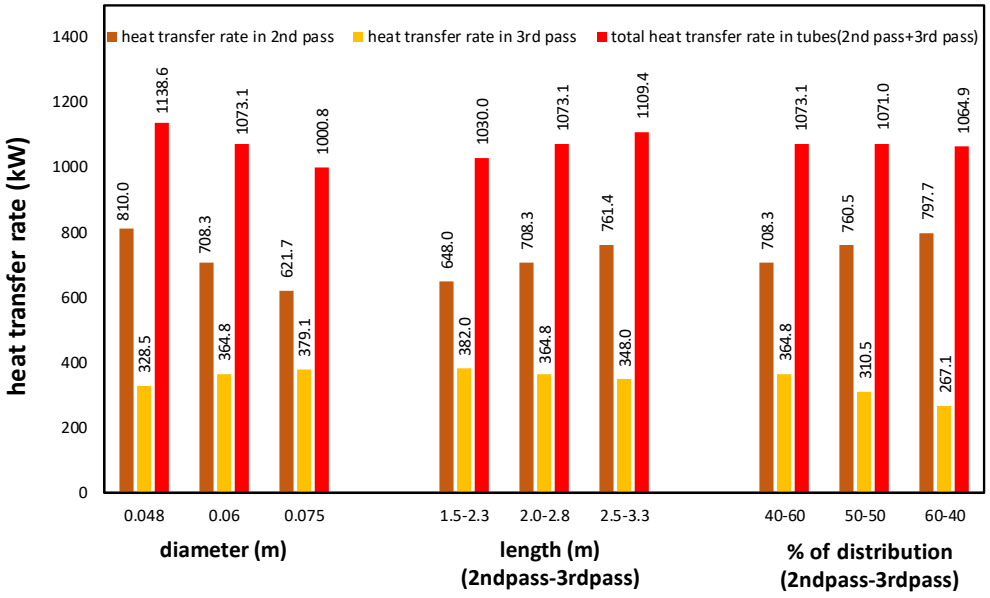

Fig. 12. Effect of tube diameter, length and distribution on heat transfer rate

Figure 13 compares the heat transfer coefficient and pressure drop of flow for changing tube diameter, length and 2nd to 3rd pass tube distribution. Fig. 13 shows that increasing tube diameter dramatically decreases the heat transfer coefficient and the pressure drop of the gas. By increasing tube diameter and maintaining tube surface area constant, tube number has decreased and the flow velocity in the tubes leads to the lower heat transfer coefficient and pressure drop and higher LMTD and temperature of the tube surface. The tube diameters are chosen based on the standard tube sizes in the market.

On the other hand, increasing tube length of the 2nd and 3rd pass of the boiler, while decreasing the tube number, causes both heat transfer coefficient and pressure drop to increase. This is caused by increasing the velocity of the combusted products in the tubes of the boiler. The results show a little change but negative effect in heat transfer coefficient and pressure drop by increasing proportion of 2nd to 3rd pass tube numbers. According to Table 2, distribution of 50-50 and 60-40 relates to the same tube diameter and length and just the tube numbers has changed. Therefore, increasing 2nd pass and decreasing 3rd pass tube numbers causes the decrease in heat transfer coefficient and increase in pressure drop. In the case of 40-60 in comparison with 50-50 distribution, tube length has decreased and 2nd pass tube numbers have increased, causing to low decrease of heat transfer coefficient and a low increase of pressure drop by the contrast effects.

Figure 14 shows steam production and total heat transfer rate for the studied cases. If the total surface of tubes remains constant, the steam production increases by increasing tube length and decreasing their number or decreasing tube diameter and increasing their number. In the constant tube diameter and length, more tube distribution in the 3rd pass relative to the 2nd one (in constant surface area), increases the total heat transfer rate and steam production. According to Fig. 14, tube diameter of 20% and a subsequent tube quantity increase, increases steam production by 3%. In addition, tube length increase of 25% in the 2nd pass and 18% in the 3rd pass, and subsequent tube quantity decrease, helps increase 1.68% steam production capacity. Tube distribution variation doesn't have a significant effect on steam generation.

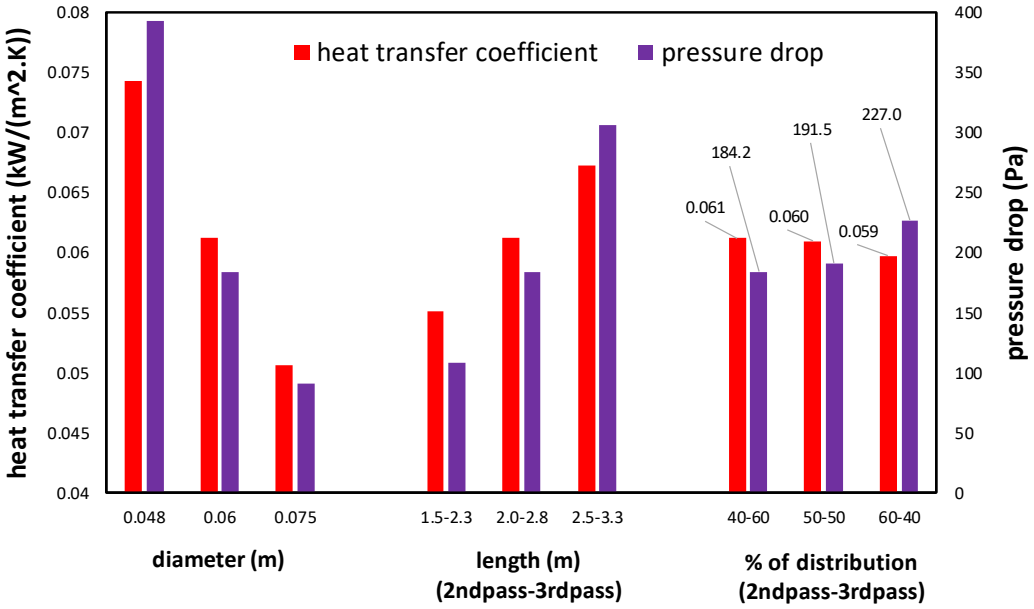

Fig. 13. Effect of tube diameter, length and distribution on heat transfer coefficient and pressure drop

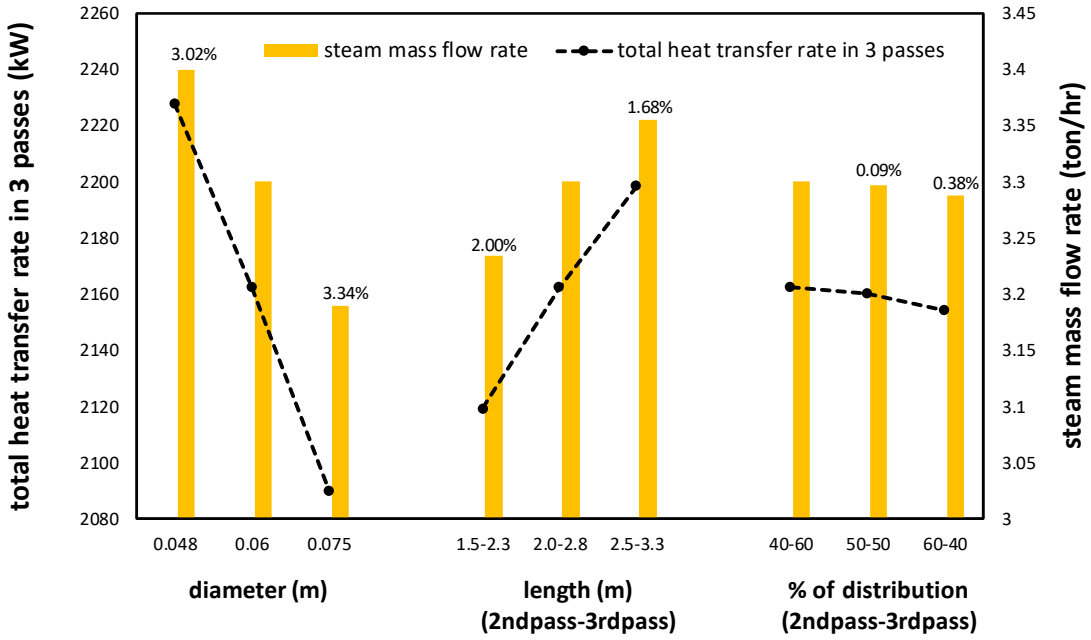

Fig. 14. Effect of tube diameter, length and distribution on total heat transfer rate and steam production

4. Conclusion

In this study, a 3-pass fire-tube boiler with a steam production of 3 ton/hr is numerically simulated. Each boiler component is modeled separately and the temperature distribution and boiler performance have been investigated. A parametric study for different diameters and length of furnace and 2nd and 3rd pass tubes, tube distribution, and burner capacity has been carried out in order to find out better performance of the boiler. The results have shown that:

- By increasing furnace surface area by increasing its diameter, length and corrugating, outlet temperature of combustion products from the boiler decreases and the heat transfer rate and steam production capacity of the boiler increase. Increasing 55% of the length and 54% of the diameter of the furnace, increases 6.56% and 1.5% of the heat transfer coefficient and steam generation.
- Bigger furnace capacity causes higher outlet temperature but higher steam production. A burner capacity increase of 33% causes 33% increase in steam generation.
- Decrease of tube diameter and increase of its quantity or increase of tube length and decrease of its quantity, decreases the outlet temperature of combustion products from the 3rd pass and increases the steam production rate.
- Reducing the diameter of the tubes by 20% and increasing the length of the tubes by 25% in the 2nd pass and 18% in the 3rd pass (with the same heat transfer surface of the tubes in pass 2 and 3), leads to steam production increase by 3% and 1.68%, respectively.
- By increasing tube distribution in the 2nd pass and decreasing the 3rd one, in comparison with the base case with distribution of 40-60% of the tubes in the 2nd and 3rd passes, the gas outlet temperature increases and therefore, heat transfer and steam generation rates decrease.

In summary, geometrical parameters of 3 passes and burner capacity are effective, but the value of burner capacity has the highest importance on boiler performance.

Fire tube boilers, besides its point-to-point calculation, need to be considered with the output emission of NOx and CO_2. This is the subject of another research of the authors to study more details of the fire tube boilers.

5. Acknowledgement

We would like to express our sincere gratitude to Damadej Espadan Company for providing the necessary support throughout the research and writing process.

References

[1] Ortiz FG. Modeling of fire-tube boilers. Applied Thermal Engineering. 2011;31(16):3463-78.

[2] Makishi O, Fujii T, Kawabe A, Tamagawa T. Measurement of the thermal resistance of scale on the inner surfaces of boiler tubes. Heat Transfer—Asian Research: Co-sponsored by the Society of Chemical Engineers of Japan and the Heat Transfer Division of ASME. 2002;31(2):117-27. https://doi.org/10.1002/htj.10020

[3] Mahmoudi M, Khorshidi Mal Ahmadi J, Zarei T. A Simultaniously Analysis of Computational Fluid Dynamics and Exergy of the Fire Tube Boiler. Journal of Petroleum Research. 2017;27(96-3):177-90.

[4] Bisetto A, Del Col D, Schievano M. Fire tube heat generators: Experimental analysis and modeling. Applied Thermal Engineering. 2015;78:236-47.

[5] Abene A, Rahmani A, Seddiki RG, Moroncini A, Guillaume R. Heat transfer study in 3-pass fire-tube boiler during a cold start-up. Software Engineering. 2018;5(4). DOI: 10.11648/j.se.20170504.11.

[6] Beyne W, Lecompte S, Ameel B, Daenens D, Van Belleghem M, De Paepe M. Dynamic and steady state performance model of fire tube boilers with different turn boxes. Applied Thermal Engineering. 2019;149:1454-62. https://doi.org/10.1016/j.applthermaleng.2018.09.103

[7] Beyne W, Daenens D, Ameel B, Van Belleghem M, Lecompte S, De Paepe M. Steady state modeling of a fire tube boiler. 2017.

[8] Khaustov SA, Zavorin AS, Buvakov KV, Sheikin VA, editors. Computer simulation of the fire-tube boiler hydrodynamics. EPJ Web of Conferences; 2015: EDP Sciences. https://doi.org/10.1051/epjconf/20158201039

[9] Lahijani AM, Supeni EE, Kalantari F. A review of indirect method for measuring thermal efficiency in fire tube steam boilers. J Ind Pollut Control. 2017;34(1):1825-32.

[10] Gaćeša B, Maneski T, Milošević-Mitić V, Nestorović MS, Petrović A. Influence of furnace tube shape on thermal strain of fire-tube boilers. Thermal science. 2014;18:S39-S47. https://doi.org/10.2298/TSCI130317172G

[11] Tognoli M, Najafi B, Rinaldi F. Dynamic modelling and optimal sizing of industrial fire-tube boilers for various demand profiles. Applied Thermal Engineering. 2018;132:341-51. https://doi.org/10.1016/j.applthermaleng.2017.12.082

[12] Tognoli M, Najafi B, Marchesi R, Rinaldi F. Dynamic modelling, experimental validation, and thermo-economic analysis of industrial fire-tube boilers with stagnation point reverse flow combustor. Applied Thermal Engineering. 2019;149:1394-407. https://doi.org/10.1016/j.applthermaleng.2018.12.087

[13] Rahmani A, Trabelsi S. Numerical investigation of heat transfer in 4-pass fire-tube boiler. American Journal of Chemical Engineering. 2014;2(5):65-70. DOI: 10.11648/j.ajche.20140205.12

[14] Kute MSB. Heat transfer enhancement in fire tube boiler using hellically ribbed tubes. 2017.

[15] Mohammadi S, Mousavi Ajarostaghi SS, Pourfallah M. The latent heat recovery from boiler exhaust flue gas using shell and corrugated tube heat exchanger: A numerical study. Heat Transfer. 2020;49(6):3797-815. https://doi.org/10.1002/htj.21809

[16] Jha R, Lele MM. Dynamic modeling of a water tube boiler. Heat Transfer. 2022;51(7):6087-121. https://doi.org/10.1002/htj.22581

[17] Morelli A, Tognoli M, Ghidoni A, Najafi B, Rinaldi F. Reduced FV modelling based on CFD database and experimental validation for the thermo-fluid dynamic simulation of flue gases in horizontal fire-tubes. International Journal of Heat and Mass Transfer. 2022;194:123033. https://doi.org/10.1016/j.ijheatmasstransfer.2022.123033

[18] Tognoli M, Keyvanmajd S, Najafi B, Rinaldi F. Simplified finite volume-based

dynamic modeling, experimental validation, and data-driven simulation of a fire-tube hot-water boiler. Sustainable Energy Technologies and Assessments. 2023;58:103321. https://doi.org/10.1016/j.seta.2023.103321

[19] Kotb A, Saad H. Simplified Applicable Model for Fire Tube Boiler. Energy and Power Engineering. 2024;16(11):359-71. DOI: 10.4236/epe.2024.1611018

[20] Pilali E, Shafiei S, Kouhikamali R, Salimi M, Amidpour M. Thermal design of fire tube boiler with superheater and estimation of temperature increase in the superheater based on machine learning methods. Energy Equipment and Systems. 2024;12(4):423-53. DOI: 10.22059/ees.2024.2030080.1467

[21] Saripalli R, Wang T, Day B. Simulation of combustion and thermal flow in an industrial boiler. 2005.

[22] Pourabdollah K. Fouling formation and under deposit corrosion of boiler firetubes. Journal of Environmental Chemical Engineering. 2021;9(1):104552. https://doi.org/10.1016/j.jece.2020.104552

[23] Magnussen BF, Hjertager BH, editors. On mathematical modeling of turbulent combustion with special emphasis on soot formation and combustion. Symposium (international) on Combustion; 1977: Elsevier.

[24] Pollhammer W, Spijker C, Six J, Zoglauer D, Raupenstrauch H. Modeling of a walking beam furnace using CFD–methods. Energy Procedia. 2017;120:477-83. DOI: 10.1016/j.egypro.2017.07.228

[25] Romero-Anton N, Huang X, Bao H, Martin-Eskudero K, Salazar-Herran E, Roekaerts D. New extended eddy dissipation concept model for flameless combustion in furnaces. Combustion and flame. 2020;220:49-62. https://doi.org/10.1016/j.combustflame.2020.06.025

[26] Coppalle A, Vervisch P. The total emissivities of high-temperature flames. Combustion and flame. 1983;49(1-3):101-8.

[27] Smith T, Shen Z, Friedman J. Evaluation of coefficients for the weighted sum of gray gases model. 1982.

[28] Yin C, Singh S, Romero SS. A gas radiation property model applicable to general combustion CFD and its demonstration in oxy-fuel combustion simulation. Energy Procedia. 2017;120:564-71. https://doi.org/10.1016/j.egypro.2017.07.213

[29] Rahmani A, Dahia A. Thermal-hydraulic modeling of the steady-state operating conditions of a fire-tube boiler. Nuclear Technology and Radiation Protection. 2009;24(1):29-37.